A DESCRIPTION OF RESULTS FROM THE "HANDBOOK ON SIGNAL FADE DEGRADATION FOR THE LAND MOBILE SATELLITE SERVICE"

Julius Goldhirsh *, **Wolfhard J. Vogel** +
* The Johns Hopkins University, APL, Laurel MD
+ The University of Texas at Austin, TX

ABSTRACT During the period 1983-88 a series of experiments were undertaken by the Electrical Engineering Research Laboratory of the University of Texas and the Applied Physics Laboratory of The Johns Hopkins University in which propagation impairment effects were investigated for the Land Mobile Satellite Service (LMSS). The results of these efforts have appeared in a number of publications, technical reports, and conference proceedings (see references). The rationale for the development of a "handbook" was to locate the salient and useful results in one single document for use by communications engineers, designers of planned LMSS communications systems, and modelers of propagation effects. Where applicable, the authors have also drawn from the results of other related investigations. We present here a description of sample results contained in this handbook which should be available in the latter part of 1990.

1. Introduction

The propagation measurement campaigns were performed in the Southern United States (New Mexico to Alabama), Virginia, Maryland, Colorado, and South-Eastern Australia. These experiments were implemented with transmitters on stratospheric balloons, remotely piloted aircraft, helicopters, and geostationary satellites (INMARSAT-B2, Japanese ETS-V, and INMARSAT Pacific). The earlier experiments were performed at UHF (870 MHz), followed by measurements at both L Band (1.5 GHz) and UHF. The satellite measurements were performed at L Band only. The general objectives of the above tests were to assess the various types of impairments to propagation caused by trees and terrain for predominantly suburban and rural regions where terrestrial cellular communication services are impractical. During these campaigns, the receiver system was located on a van outfitted with UHF (870 MHz) and L Band (1.5 GHz) antennas on its roof, and receivers and data acquisition equipment in its interior.

The major LMSS related topics reviewed in the "handbook" are: [1] Attenuation due to individual trees - static case, [2] Attenuation due to roadside trees-mobile case, [3] Signal degradation for line of sight communications, [4] Fade, non-fade duration and phase spread, and [5] Cross polarization, antenna directivity, and space diversity effects. In the following paragraphs we present an overview of results for items [2] and [5] in order to provide a "flavor" of the handbook contents and to examine material not detailed previously.

2. Attenuation Due to Roadside Trees - Dynamic Case

2.1 Empirical Roadside Shadowing Model

Cumulative fade distributions were systematically derived from helicopter-mobile [Goldhirsh and Vogel; 1987, 1989] and satellite-mobile measurements [Vogel and Goldhirsh, 1990] in the Central Maryland region. This formulation is referred to as the "Empirical Roadside Shadowing (ERS)" model. It may be described as follows for P = 1 to 20%

$$F(P,\theta) = -M(\theta)\ln P + B(\theta) \tag{1}$$

where F(P,θ) is the fade in dB, P is the percentage of distance (or time) the fade is exceeded, and θ is the path elevation angle to the satellite. Least square fits of second and first order polynomials in elevation angle θ (deg) generated for M and B, respectively, result in

$$M(\theta) = a + b\theta + c\theta^2 \tag{2}$$

$$B(\theta) = d\theta + e \tag{3}$$

where

$$\begin{cases} a = 3.44 \quad b = .0975 \\ c = -0.002 \quad d = -0.443 \quad e = 34.76 \end{cases} \tag{4}$$

In Figure 1 are given a family of cumulative distributions (percentage versus fade exceeded) for the indicated path elevation angles.

2.2 L-Band Versus UHF Attenuation Scaling Factor–Dynamic Case

Simultaneous mobile fade measurements by Goldhirsh and Vogel [1987, 1989] at L-Band (1.5 GHz) and UHF (870 MHz) have demonstrated that the ratio of fades at equal probability levels is approximately consistent with the square root of the ratio of frequencies over this frequency interval. More specifically, we observed that for f_L = 1.5 GHz and f_{UHF} = 870 MHz

$$F(f_L) \approx 1.31F(f_{UHF}) \tag{5}$$

where the multiplying coefficient 1.31 was shown to have an rms deviation of +/- 0.1 over a fade exceedance range from 1% to 30%.

2.3 Seasonal Effects–Dynamic Case

Seasonal measurements were performed by the authors for the dynamic case in which the vehicle was traveling along a tree-lined highway in Central Maryland (Route 295) along which the propagation path was shadowed over approximately 75% of the road distance [Goldhirsh and Vogel;1987, 1989]. Cumulative fade distributions were derived for March 1986 during which the deciduous trees were totally without foliage. These were compared with similar distributions acquired in October 1985 and June 1987, during which the trees were approximately in 80% and full blossom stages, respectively. For the frequency f = 870 MHz and P = 1% to 30%

$$F(\text{full foliage}) = 1.24F(\text{no foliage}) \tag{6}$$

3. Cross Polarization

By making repeated measurements at co- and cross-polarization for selected runs during the Australian campaign, equi-probability "cross-polar isolation levels, CPI" were determined. The CPI is defined by

$$\mathrm{CPI(P)} = \frac{\mathrm{COPS(P)}}{\mathrm{CRPS(P)}} \tag{7}$$

where COPS and CRPS represent the co-polarization and cross-polarization signal levels at the equi-probability level of fade exceedance, P. The CPI (in dB) was found to follow the linear relation,

$$\mathrm{CPI} = -1.605\mathrm{F} + 18.94 \tag{8}$$

where F is the co-pol fade (in dB).

The rms deviation between the "best fit linear" relation (8) and the data points for the corresponding runs was 0.4 dB. We note from the plot in Figure 2 that the isolation severely degrades as a function of fade level. Hence, the simultaneous employment of co- and cross-polarized transmissions in a "frequency re-use" system is implausible because of poor isolation caused by multi-path scattering into the cross-polarized channel.

4. Effect of Antenna Directivity on Fade Distributions

During the Australian campaign, a number of repeated runs were implemented in which high and low gain antennas were employed. The characteristics of these antennas are given in Table 1. Figure 3 shows a plot of the high gain receiver fade versus the low gain fade over the low gain fade interval of 1 to 15 dB. The data points were found to follow the linear relation

$$\mathrm{F(HG)} = 1.133 * \mathrm{F(LG)} + 0.51 \tag{9}$$

where F(HG) and F(LG) represent the high and low gain fades (in dB), respectively. Agreement between the relation (9) and the data points for F(HG) were within 0.2 dB rms.

We note that the high gain system experiences consistently more fading than the low gain case. For example at 3 and 14.5 dB (of low gain fades), the high gain fades are 4 and 17 dB, respectively, which represent 33% and 17% increases. This slight increase in attenuation for the high gain case occurs because less average power is received via multi-path through the associated narrower antenna beam. On the other hand, the azimuthally omni-directional low gain antenna receives more scattered multi-path contributions resulting in an enhanced averaged received power. It is important to note that because the more directive antenna has a 10 dB higher gain associated with it, the net power received by it is still significantly higher than that received for the less directive antenna. Even at the 15 dB fade level (low gain receiver system), the net received power for the more directive antenna system is larger by 7.5 dB.

5. Diversity Operation

A space diversity simulation has been carried out employing the data base corresponding to approximately 400 km of roadside tree shadowing measurements taken during the Australian campaign [Vogel, Goldhirsh, and Hase; 1989]. Space diversity operation for the LMSS may be envisaged by the scenario of two spaced antennas mounted atop a vehicle where each antenna is fed to a separate receiver system. Because the signal levels at the two separated antennas are likely to be different at any instant of time, rapid switching between the two receiver outputs followed by subsequent processing enable the larger signal to be accessed. Such a dual antenna system should therefore require smaller fade margins for the same driving distance than single terminal operation.

5.1 Joint Probabilities

In Figure 4 are depicted a family of cumulative fade distribution functions derived from the above mentioned simulation. The curve labeled d = 0 represents the single terminal cumulative fade distribution corresponding to the data base described above. The curves labeled d = 1 to 10 m represent the individual joint probability cumulative fade distribution for the indicated antenna separations. Such a distribution represents "the joint probability that two antennas spaced a distance d mutually exceed the abscissa value of fade." We note that the joint probabilities tend to coalesce with increasing antenna separation. That is, the fade distributions for 8 m and 10 m separation show insignificant differences.

5.2 Diversity Improvement Factor

A convenient descriptor for characterizing the improvement in communications for a space diversity configuration is the "Diversity Improvement Factor, DIF" defined by

$$\mathrm{DIF}(F,d) = \frac{P_o(F)}{P_d(F)} \tag{10}$$

where $P_o(F)$ represents the single terminal probability distribution at the fade depth F, and $P_d(F)$ represents the joint probability distribution for an antenna spacing d assuming the same attenuation F is exceeded. We note from Figure 4 that DIF(8,1) $\approx$ 3, which implies that when the antennas are separated 1 m, the equivalent time over which the fade margin of 8 dB is exceeded is three times greater for the single terminal system as compared to diversity pair operation. Hence, assuming an 8 dB fade margin and a 6 minute "down time" for the single terminal case, the outage for the diversity system would only be 2 minutes.

A least square estimate of DIF was derived given by,

$$\mathrm{DIF}(d,F) = 1 + [0.2 \times \ln(d) + 0.23] \times F \tag{11}$$

where d is the antenna separation expressed in m and F is the fade depth in dB. In Figure 5 are plotted a family of curves depicting DIF as a function of fade depth for antenna separations between 1 and 10 m. We note that at the larger separations for any given fade depth, the rate at which DIF increases diminishes rapidly.

5.3 Diversity Gain

The "diversity gain, DG" is a concept defined by Hodge [1978] for an earth- satellite communications system involving two spaced antennas operating in a diversity mode in the presence of precipitation. This concept may also be applied to space diversity operation for the LMSS case as described above. The diversity gain is defined as the fade reduction experienced while operating in the diversity mode at a given exceedance. It is equal to the difference in fades between the single terminal and joint probability distributions at a fixed exceedance level. For example, gleaning Figure 4, we note that the diversity gain at an exceedance of 1% for a 1 m antenna separation is 4 dB. Hence, while the single terminal operation at a 1% exceedance will experience a 12 dB fade, the fade for diversity operation with a 1 m antenna separation is only 8 dB.

In Figure 6 is plotted the diversity gain versus antenna separation for a family of single terminal fade levels. Each single terminal fade uniquely defines an exceedance level. For example, an 8 dB fade occurs at an exceedance level of 3% as is noted from Figure 4. Figure 6 shows that the effect of the antenna separation is dramatic the first 2 meters, beyond which relatively little fade reduction ensues for larger spacings.

5.4 Caveats

Although the above results pertaining to space diversity operation appears inviting, two major caveats must be borne in mind. One, signal fluctuations normally occur rapidly. For example, fade duration statistics derived by Hase, Vogel, and Goldhirsh [1990] have demonstrated that at a fade threshold of 5 dB, the median fade duration distance is 0.5 m. Assuming a nominal driving speed of 25 m/s, a typical switching rate of 20 ms is required. Secondly, there is the added cost for an additional antenna-receiver-processor system.

References

Goldhirsh, J. and W. J. Vogel, "Roadside Tree Attenuation Measurements at UHF for Land-Mobile Satellite Systems," *IEEE Trans. Antennas Propagat.*, AP-35, pp 589–596, 1987.

Goldhirsh, J. and W. J. Vogel., "Mobile Satellite System Fade Statistics for Shadowing and Multipath from Roadside Trees at UHF and L-band," *IEEE Trans. Antennas Propagat.*, AP–37, pp 489–498, 1989.

Hase, Y. W. J. Vogel, and J. Goldhirsh, "Fade-Durations Derived from Land-Mobile Satellite Measurements in Australia," *IEEE Trans. on Commun.*, (in press), 1990.

Hodge, D. B., "Path Diversity for Earth-Space Communication Links,"*Radio Sci.*, Vol 13, No 3, pp. 481–487, 1978.

Vogel, W. J., and J. Goldhirsh, "Tree Attenuation at 869 MHz Derived from Remotely Piloted Aircraft Measurements," *IEEE Trans. Antennas Propagat.*, AP-34, pp 1460–1464, 1986.

Vogel, W. J., and J. Goldhirsh, "Mobile Satellite System Propagation Measurements at L-Band Using MARECS-B2," *IEEE Trans. Antennas Propagat.*, AP–38, pp 259–264, 1990.

Vogel, W. J., and J. Goldhirsh ., "Fade Measurements at L-band and UHF in Mountainous Terrain for Land Mobile Satellite Systems," *IEEE Trans. Antennas Propagat.*, vol. AP-36, pp 104–113, 1988.

Vogel, W. J., J. Goldhirsh, and Y. Hase., "Land-Mobile-Satellite Propagation Measurements in Australia Using ETS-V and INMARSAT-Pacific," *APL/JHU Tech. Rep. S1R89U-037*, 1989 (Laurel, MD; The Johns Hopkins University, Applied Physics Laboratory).

Table 1: Summary of pertinent characteristics for high and low gain receiver antennas used during the Australian campaign [Vogel, Goldhirsh, and Hase: 1989].

Characteristics	Low Gain	High Gain
Type	Crossed Drooping Dipoles	Helix
Gain(dB)	4	14
Nominal Pattern (El)	15° - 70° (fixed)	45° (Principal Planes)
Nominal Pattern (Az)	omni-directional	45°
Polarization	RHCP or LHCP	RHCP or LHCP

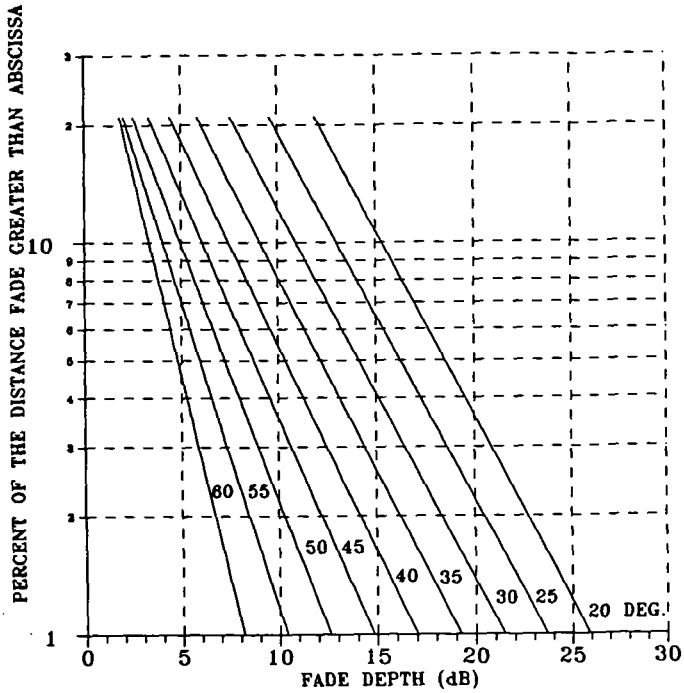

Figure 1: Empirical Roadside Shadowing (ERS) model giving cumulative fade distributions for a family of path elevation angles.

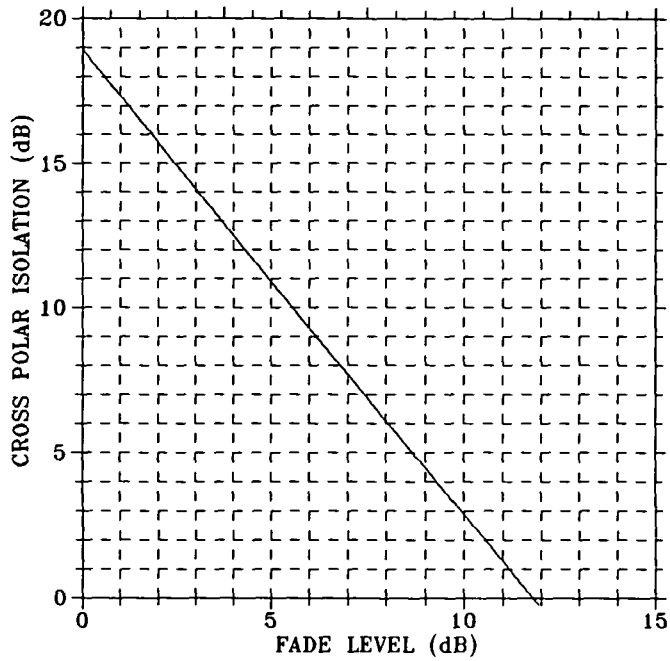

Figure 2: Cross-Polarization Isolation (CPI) as a function of fade depth.

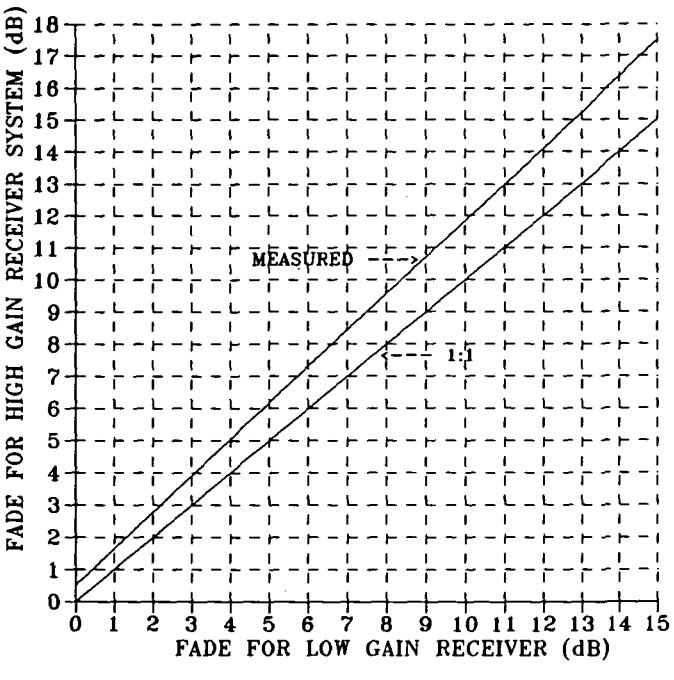

Figure 3: Fades derived from high gain versus low gain antenna systems for roadside shadowing.

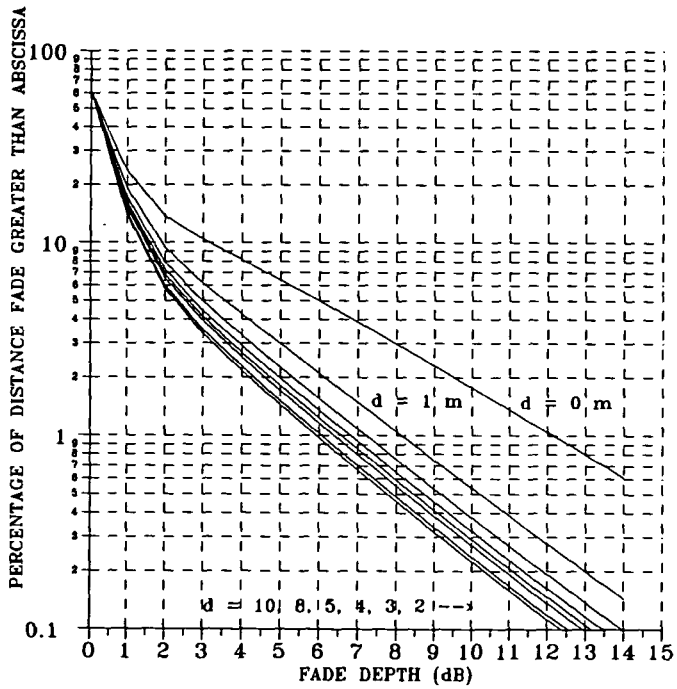

Figure 4: Family of joint probability distributions for various antenna separations corresponding to roadside shadowing.

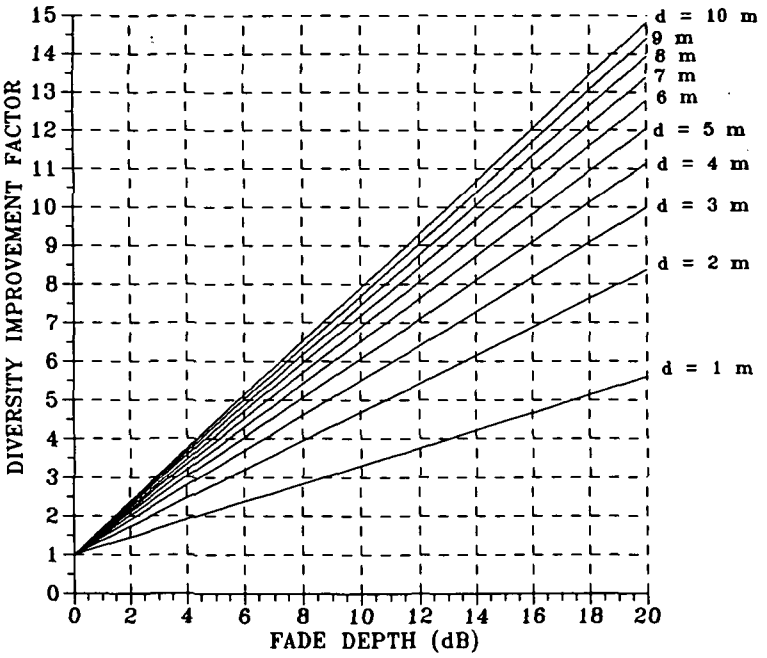

Figure 5: Family of Diversity Improvement Factors (DIF) as a function of fade for various antenna separations.

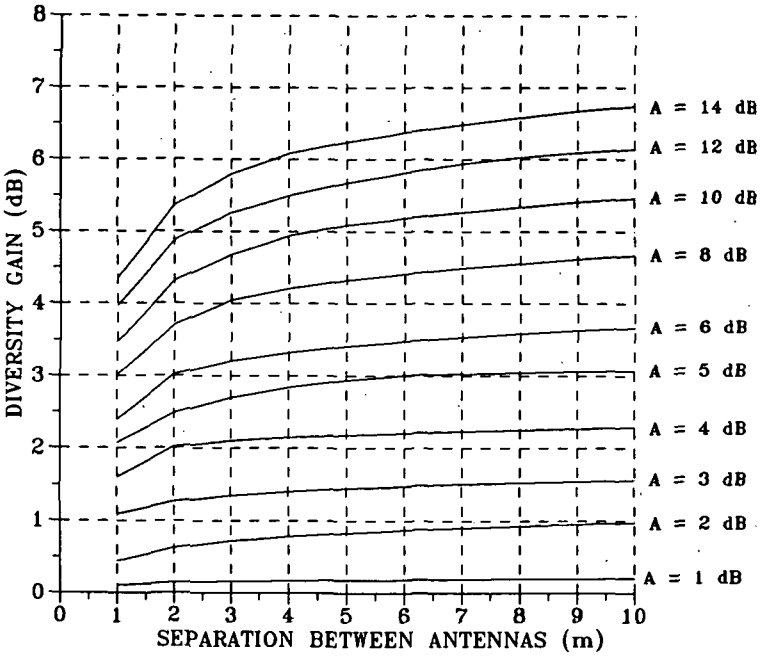

Figure 6: Family of Diversity Gains (DG) versus antenna separations for various single terminal fade depths.